

Enhanced pair production in strong fields by multiple-slit interference effect with dynamically assisted Schwinger mechanism

Z. L. Li,¹ D. Lu,¹ B. S. Xie,^{1,*} L. B. Fu,² J. Liu,² and B. F. Shen³

¹Key Laboratory of Beam Technology and Materials Modification of the Ministry of Education, College of Nuclear Science and Technology, Beijing Normal University, Beijing 100875, China

²National Laboratory of Science and Technology on Computational Physics, Institute of Applied Physics and Computational Mathematics, Beijing 100088, China

³Shanghai Institute of Optics and Fine Mechanics, Chinese Academy of Sciences, Shanghai 201800, China
(Received 13 March 2014; revised manuscript received 9 April 2014; published 13 May 2014)

In the quantum kinetic framework, we investigate the momentum spectrum and the number density of created electron-positron pairs from vacuum in the combined electric fields composed of two sets of alternating-sign electric field pulse trains, a strong but slowly varying one and a weak but rapidly changing one. It is found that the pair production can be strongly enhanced by combining the multiple-slit interference effect with the dynamically assisted Schwinger mechanism. By considering the contribution of the transverse momentum, we find that the number density of created particles depends linearly on the electric field pulse number, i.e., a power law with index 1. Moreover, we study the effect of interpulse time delay on pair production and find that the number density is very sensitive to the interpulse time delay. The symmetry of the momentum spectrum for an N -pulse electric field and the difference of the multiple-slit interference effect between the nonperturbative Schwinger mechanism and the perturbative multiphoton electron-positron pair creation are also studied. Some possible explanations for observed results of momentum spectrum and number density are also given and discussed.

DOI: 10.1103/PhysRevD.89.093011

PACS numbers: 12.20.Ds, 02.60.Nm, 11.15.Tk

I. INTRODUCTION

A vacuum in the presence of a strong electric field breaking down by emitting electron-positron (EP) pairs is a well-known theoretical prediction of QED [1,2]. For a constant electric field, the EP pair production rate was first calculated by Schwinger [3], and the critical electric field strength was given as $E_{\text{cr}} = m^2/e \sim 1.32 \times 10^{16}$ V/cm, where m is the electron mass and e is the positron charge (the units $\hbar = c = 1$ are used). Because of the contribution of Schwinger, the nonperturbative EP pair production is also called the Schwinger mechanism. Although many theoretical works of this nonperturbative mechanism have been done [4–12], an experimental observation is still absent because the very high critical electric field gives rise to an exponential suppression of EP pair production for $E \ll E_{\text{cr}}$, according to the Schwinger formula [3].

With the developments of laser technology, particularly the chirped pulse amplification technique, the laser field in ultrahigh intensity laser facilities, such as the extreme light infrastructure [13] and x -ray free electron laser [14], may approach to the subcritical field strength, i.e., $E \sim 0.1E_{\text{cr}}$. This attracts much attentions to realize an experimental observation of EP pair production from a vacuum again [15,16]. To achieve this goal, enhancing EP pair production

by optimizing the shape of laser pulses is proposed for future experiments [17–22].

In Ref. [17], the authors studied the dynamically assisted Schwinger mechanism (DASM). They found that the EP pair creation could be strongly enhanced by superimposing a weak and rapidly changing electric field on a strong and slowly varying one. It is known that the DASM was first studied by superposing two simple Sauter-like electric fields [17,23,24]. But a realistic laser pulse field [25] is more complex and makes the worldline instanton technique used in Ref. [17] invalid. Fortunately, this mechanism can be easily investigated by a quantum kinetic method. By numerically solving the quantum Vlasov equation (QVE), more complex combined electric fields were studied in Ref. [26], and an optimal control theory was also tried recently [27]. Furthermore, the quantum kinetic method can calculate not only the number density but also the momentum distribution of created particles.

Another route to achieve the detection of EP pair production is suggested by Akkermans and Dunne [28], i.e., the time-domain multiple-slit interference effect. They found that the value of the central momentum distribution function for an alternating-sign N -pulse electric field is N^2 times that for a single-pulse electric field. In our recent work [29], the relationship between the number density of created particles and the pulse number of the electric field is investigated for zero transverse momentum. It is shown that the number density of created pairs grows with the pulse

*Corresponding author.
bsxie@bnu.edu.cn.

number N . For more details about the study of the multiple-slit interference effect by solving the QVE, see Ref. [30].

In this paper, in a quantum kinetic framework, we focus study on the enhanced EP pair production by combining the multiple-slit interference effect with the DASM for both zero transverse momentum and full momentum space. The momentum spectrum of created particles and the relationship between the number density and the pulse number for the electric fields composed of a strong and slowly varying alternating-sign electric-field pulse train and a weak and rapidly changing one are studied. Furthermore, the effects of both the interpulse time delay and the electric field time interval on the particle number density are also considered.

This paper is organized as follows. In Sec. II, we briefly introduce the quantum Vlasov equation. In Sec. III, by numerically solving the QVE, we study the strongly enhanced EP pair production in the presence of a combined alternating-sign electric-field pulse train for both zero transverse momentum space and full momentum space. Section IV gives the conclusions and some discussions for our results.

II. QUANTUM VLASOV EQUATION

In the subcritical field regime $E \lesssim 0.1E_{\text{cr}}$, the number of created pairs and the backreaction electric current are so small that the collision effect and the internal electric field can be ignored. Since the spatial focusing scales of the laser pulse are larger than the electron Compton wavelength, i.e., the spatial scales for EP pair production, the spatial variation of the background laser field is not considered. By considering a standing-wave field produced by two counterpropagating laser pulses, the magnetic effects can be neglected as well, i.e., $\mathbf{B}(t) = 0$. Therefore, the background laser field is a spatially homogeneous and time-dependent electric field $\mathbf{E}(t) = (0, 0, E(t))$. Using the temporal gauge $A_0(t) = 0$, the spatially uniform and time-varying vector potential becomes $A_\mu(t) = (0, 0, 0, A(t))$ with $E(t) = -\dot{A}(t)$.

From the Dirac equation in a uniform and time-varying electric field and employing a canonical time-dependent Bogoliubov transformation, one can derive the following integrodifferential equation about the single particle momentum distribution function $f(\mathbf{k}, t)$, i.e., QVE (for more details, see Ref. [8]),

$$\frac{df(\mathbf{k}, t)}{dt} = \frac{1}{2} \frac{eE(t)\varepsilon_\perp}{\omega^2(\mathbf{k}, t)} \int_{t_0}^t dt' \frac{eE(t')\varepsilon_\perp}{\omega^2(\mathbf{k}, t')} [1 - 2f(\mathbf{k}, t')] \times \cos \left[2 \int_{t'}^t d\tau \omega(\mathbf{k}, \tau) \right], \quad (1)$$

where e is the magnitude of the electron charge, $\mathbf{k} = (\mathbf{k}_\perp, k_\parallel)$ is the canonical momentum, $\varepsilon_\perp^2 = m^2 + \mathbf{k}_\perp^2$ denotes the transverse energy squared, m is the electron mass, $\omega^2(\mathbf{k}, t) = \varepsilon_\perp^2 + k_\parallel^2(t)$ represents the total energy

squared, and $k_\parallel(t) = k_\parallel - eA(t)$ is defined as the kinetic momentum along the electric field $E(t)$. From the right-hand side of Eq. (1), one can see the effect of quantum statistics on EP pair production via the Pauli-blocking factor “[$1 - 2f(\mathbf{k}, t')$].” Moreover, the non-Markovian character for EP pair production is also presented because the Pauli-blocking factor depends on the history of the distribution function and the term “cos” depends on the history of the electric field. One should also note that the single particle momentum distribution function $f(\mathbf{k}, t)$ describes the created real particles only when the external electric field becomes zero at $t \rightarrow +\infty$. Thus, we are just interested in the distribution function $f(\mathbf{k}, +\infty)$ and the particle number density $n(+\infty)$.

By introducing $W(\mathbf{k}, t) = eE(t)\varepsilon_\perp/\omega^2(\mathbf{k}, t)$ and $\Theta(\mathbf{k}, t', t) = \int_{t'}^t d\tau \omega(\mathbf{k}, \tau)$, Eq. (1) can be reduced to

$$\frac{df(\mathbf{k}, t)}{dt} = \frac{1}{2} W(\mathbf{k}, t) \int_{t_0}^t dt' W(\mathbf{k}, t') [1 - 2f(\mathbf{k}, t')] \times \cos[2\Theta(\mathbf{k}, t', t)]. \quad (2)$$

To numerically solve Eq. (2), two auxiliary quantities are introduced as

$$u(\mathbf{k}, t) = \int_{t_0}^t dt' W(\mathbf{k}, t') [1 - 2f(\mathbf{k}, t')] \times \cos[2\Theta(\mathbf{k}, t', t)], \quad (3)$$

$$v(\mathbf{k}, t) = \int_{t_0}^t dt' W(\mathbf{k}, t') [1 - 2f(\mathbf{k}, t')] \times \sin[2\Theta(\mathbf{k}, t', t)]. \quad (4)$$

Then, Eq. (2) can be equivalently transformed into the following first-order ordinary differential equations:

$$\frac{df(\mathbf{k}, t)}{dt} = \frac{1}{2} W(\mathbf{k}, t) u(\mathbf{k}, t), \quad (5)$$

$$\frac{du(\mathbf{k}, t)}{dt} = W(\mathbf{k}, t) [1 - 2f(\mathbf{k}, t)] - 2\omega(\mathbf{k}, t) v(\mathbf{k}, t), \quad (6)$$

$$\frac{dv(\mathbf{k}, t)}{dt} = 2\omega(\mathbf{k}, t) u(\mathbf{k}, t). \quad (7)$$

Finally, we can get the single particle momentum distribution function $f(\mathbf{k}, t)$ by solving Eqs. (5)–(7) with the initial conditions $f(\mathbf{k}, -\infty) = u(\mathbf{k}, -\infty) = v(\mathbf{k}, -\infty) = 0$. Then, the number density of created particles evolving over time can be obtained by integrating $f(\mathbf{k}, t)$ to momentum as

$$n(t) = 2 \int \frac{d^3k}{(2\pi)^3} f(\mathbf{k}, t), \quad (8)$$

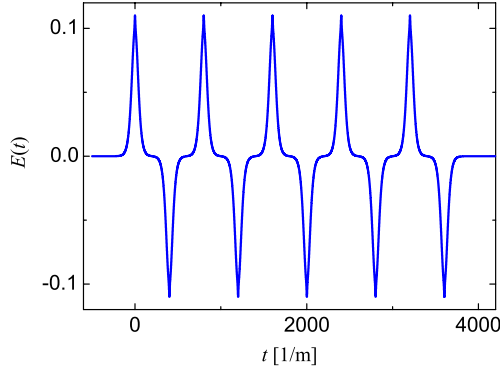


FIG. 1 (color online). The combined electric field $E(t)$ with $N = 10$. The electric field parameters are chosen as $E_1 = 0.1$, $\omega_1 = 0.02$, $E_2 = 0.01$, $\omega_2 = 0.22$, $\tau = 400.3$, and $T = 0$.

where the factor 2 comes from the degeneracy of electrons. In this paper, we focus on the particle distribution function $f(\mathbf{k}, +\infty)$ and the particle number density $n(+\infty)$.

III. NUMERICAL RESULTS

In this section, we show the numerical results of EP pair production through combining the multiple-slit interference effect with the DASM in the presence of the electric field

$$\begin{aligned}
 E(t) &= E_1(t) + E_2(t) \\
 &= \sum_{i=0}^{N-1} (-1)^i E_1 \operatorname{sech}^2[\omega_1(t - i \cdot \tau_1)] \\
 &\quad + \sum_{i=0}^{N-1} (-1)^i E_2 \operatorname{sech}^2[\omega_2(t - i \cdot \tau_2 + T)], \quad (9)
 \end{aligned}$$

where $E_1(t)$ is a strong and slowly varying alternating-sign electric-field pulse train, $E_2(t)$ is a weak and rapidly changing one, N indicates the electric-field pulse number, E_1 and E_2 are the electric-field strength, ω_1 and ω_2 represent the inverse-time width scale, $\tau_1 = \tau_2 \equiv \tau$ is the time delay between the electric-field pulses, and T is the time interval between the electric fields $E_1(t)$ and $E_2(t)$. For convenience, we choose $E_1 = 0.1$, $\omega_1 = 0.02$, $E_2 = 0.01$, and $\omega_2 = 0.22$. A typical combined field $E(t)$ is plotted in Fig. 1.

A. Momentum space for $\mathbf{k}_\perp = 0$

First, we study the EP pair production for zero transverse momentum in the combined electric field $E(t)$. The longitudinal momentum spectra for the electric field $E(t)$ with different pulse numbers are shown in Fig. 2. Here, the pulse number N is chosen as 1, 2, 3, and 10. It is clear to see that the interference effect is very obvious, and the distribution function at the central momentum for the N -pulse electric field is still N^2 times that for the single-pulse electric field. These results are the same as in Ref. [28].

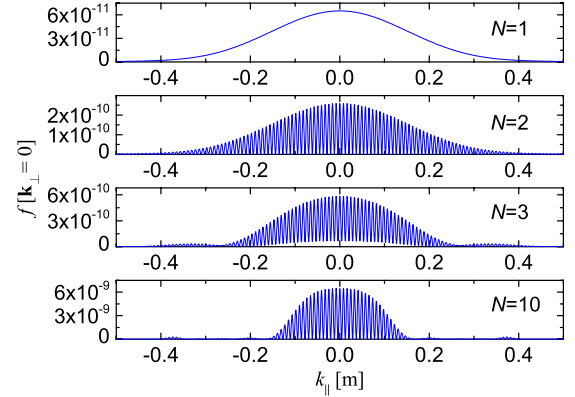


FIG. 2 (color online). The longitudinal momentum spectra for the combined electric field $E(t)$ with different electric-field pulse numbers N , i.e., $N = 1, 2, 3$, and 10 . The electric field parameters are the same as in Fig. 1.

However, to our knowledge, the longitudinal momentum spectrum for odd-pulse electric field, e.g., $N = 3$, is not reported before. It can be observed that an important difference, compared to the momentum spectrum of the even-pulse electric field, exists for the small longitudinal momentum of the $N = 3$ case, in which the local minima of the momentum distribution function $f[\mathbf{k}_\perp = 0]$ are larger than zero. From the point of view of the quantum scattering picture, it indicates that the perfect transmission is not possible for any small momentum. Note that the difference can also be seen from the approximate expression of Eq. (13) in Ref. [28]. Moreover, we find that when the pulse number N increase, the longitudinal momentum region in which dominant pair production occurs becomes

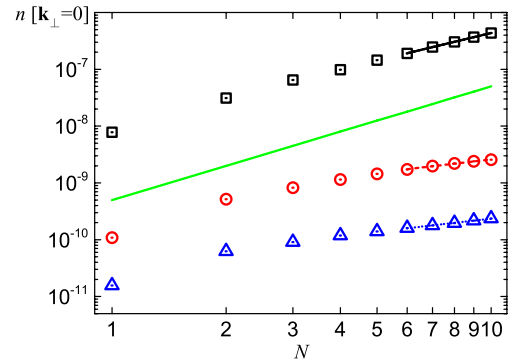


FIG. 3 (color online). The number density of created pairs $n[\mathbf{k}_\perp = 0]$ as a function of the electric field pulse number N , for the electric field $E_1(t)$ (blue triangles), the electric field $E_2(t)$ (red circles), and the combined electric field $E(t)$ (black squares), respectively. The dotted blue, dashed red, and solid black lines are the fitted ones for $E_1(t)$, $E_2(t)$, and $E(t)$ with the slopes ~ 0.758 , 0.775 , and 1.609 , respectively. The solid green line is a reference one as $n[\mathbf{k}_\perp = 0] \propto N^2$. The electric field parameters are the same as in Fig. 1.

small. In fact, this result also holds for the full momentum space of pair production.

Now, let us consider the relationship between the number density of created particles $n[\mathbf{k}_\perp = 0]$ and the electric-field pulse number N . The result is depicted in Fig. 3 for the electric field $E_1(t)$ (blue triangles), the electric field $E_2(t)$ (red circles), and the combined electric field $E(t)$ (black squares), respectively. The dotted blue, dashed red, and solid black lines are the fitted ones for $E_1(t)$, $E_2(t)$, and $E(t)$ with the slopes ~ 0.758 , 0.775 , and 1.609 , respectively. A reference solid green line $n[\mathbf{k}_\perp = 0] \propto N^2$ is also plotted. We can see that, with the electric-field pulse number N increasing from 1 to 10, the number density of created particles increases from 1.57×10^{-11} to 2.36×10^{-10} , 1.09×10^{-10} to 2.56×10^{-9} , and 7.80×10^{-9} to 4.35×10^{-7} for the electric fields $E_1(t)$, $E_2(t)$, and $E(t)$, respectively. The relationship between the number density and the pulse number N is complex and different from that between the central momentum distribution function and the pulse number. From the slope of the fitted lines, however, we find that for large N they are approximately the power laws with the different index as ~ 0.758 , 0.775 , and 1.609 for $E_1(t)$, $E_2(t)$, and $E(t)$, respectively. Moreover, we can also see that the number of created particles can be greatly enhanced by combining the multiple-slit interference effect with the DASM. This result indicates that, to get a high particle number density, combining the interference effect with the DASM is better than simply adding the pulse number [29]. Thus, we hope that this result is helpful to observe the EP pair production effectively for future experiments.

Additionally, the effect of the interpulse time delay between the electric field pulses on the number density of created particles is worthwhile to be considered as well. Figure 4 shows the number density of created pairs $n[\mathbf{k}_\perp = 0]$ as a function of the interpulse time delay τ for the combined electric field $E(t)$ with $N = 10$. One can see that the number density is very sensitive to the

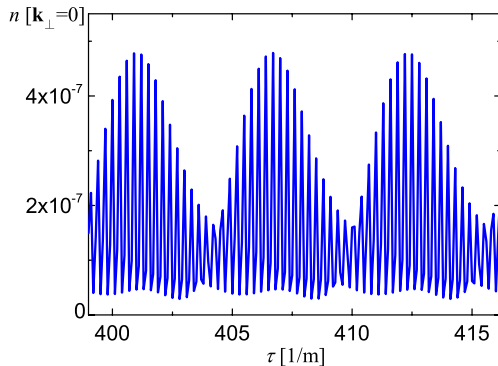


FIG. 4 (color online). The number density of created particles $n[\mathbf{k}_\perp = 0]$ as a function of the interpulse time delay τ for the combined electric field $E(t)$ with $N = 10$. The electric field parameters are chosen as $E_1 = 0.1$, $\omega_1 = 0.02$, $E_2 = 0.01$, $\omega_2 = 0.22$, and $T = 0$.

interpulse time delay τ , and there is a quasiperiodical dependency between them. The similar results can also be seen in Fig. 2 of Ref. [27], and the origin of this quasiperiodical structure is discussed as to be caused by some kind of resonance effect. However, it is more complex for our results here because we consider a combined electric field instead of a simple weak and rapidly changing one. Therefore, the quasiperiodical structure may be related to both multiphoton absorption and quantum tunneling. This structure can also be understood in the point of view of the quantum mechanical scattering picture. Based on the similarity between spinor QED and scalar QED [29,31,32] and for the sake of simplicity, we shall discuss the scattering problem in scalar QED. As in Refs. [31,32], vacuum pair production can be regarded as a one-dimensional over-the-barrier scattering problem in the time domain with the positive energy $m^2 + \mathbf{k}_\perp^2$ and the negative potential $-[k_\parallel - eA(t)]^2$. Note that the square of the absolute value of the reflection coefficient is approximate to the momentum distribution function of created particles for $E \ll E_{\text{cr}}$. In our case, the negative potential is a finite periodic potential, and its shape depends on the interpulse time delay τ and the longitudinal momentum k_\parallel . For a given energy, both τ and k_\parallel with a suitable value will give rise to a perfect transmission [33] and form the resonance effect. For instance, the oscillations of longitudinal momentum spectra in Fig. 2 show the resonance induced by k_\parallel with fixed τ while the standard Fabry–Perot form depicted in Fig. 4 of Ref. [28] shows the resonance caused by τ with fixed k_\parallel . Hence, the quasiperiodic structure of the particle number density is the contribution of both the resonance caused by the interpulse time delay and that caused by the longitudinal momentum. We think the above analysis is also valid for spinor QED even if it will be a little more complex. Moreover, in Fig. 4, we can also find that the number density varies within 1 order of magnitude.

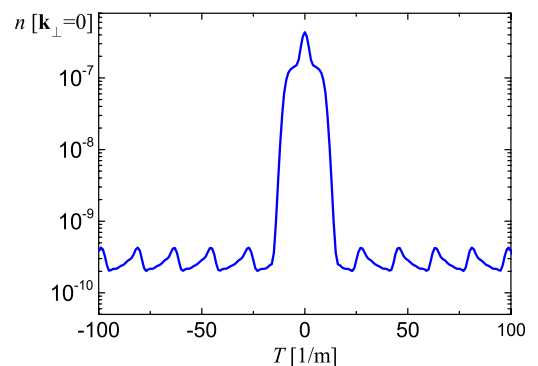


FIG. 5 (color online). The number density of created particles $n[\mathbf{k}_\perp = 0]$ as a function of the electric-field time interval T for the combined electric field $E(t)$ with $N = 10$. The electric-field parameters are chosen as $E_1 = 0.1$, $\omega_1 = 0.02$, $E_2 = 0.01$, $\omega_2 = 0.22$, and $\tau = 400.3$.

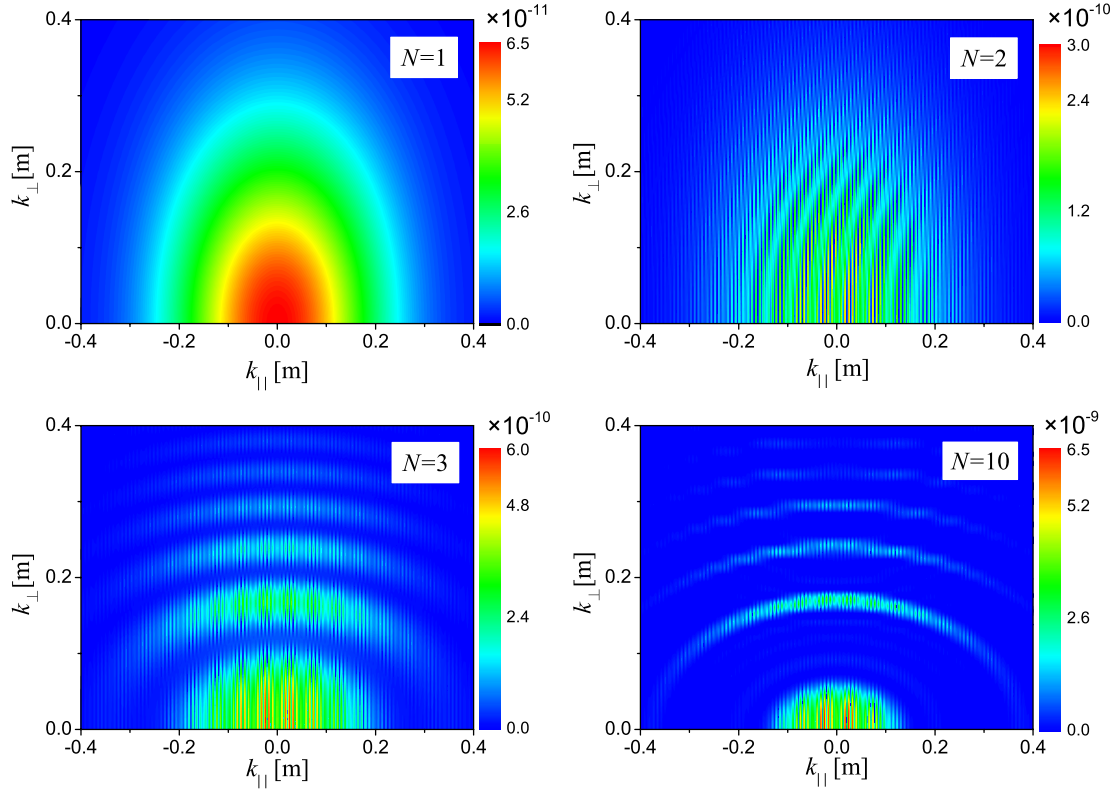


FIG. 6 (color online). The momentum spectra for the combined electric field $E(t)$ with different electric-field pulse numbers N , i.e., $N = 1, 2, 3$, and 10 . The electric-field parameters are the same as in Fig. 1.

The number density of created pairs $n[\mathbf{k}_\perp = 0]$ as a function of the electric field time interval T for the combined electric field $E(t)$ with $N = 10$ is shown in Fig. 5. We find that the number density is also sensitive to the electric field time interval T , and there is a great change of the number density for small $|T|$ and a periodical change for large $|T|$. These results reveal the features of nonlinear dependency of the total energy $\omega(\mathbf{k}, t)$ on the longitudinal momentum and the external electric field. They can also be understood from the viewpoint of the aforementioned scattering problem. For a fixed interpulse time delay, the shape of the effective potential depends on the electric-field time interval T and the longitudinal momentum k_\parallel . Thus, the sensitivity of number density on T is the result of resonance effect from both T and k_\parallel . In addition, we find that the number density is an even function of the electric-field time interval T and reaches its maximum value at $T = 0$. This is related to the symmetry between the combined electric field for positive T and that for negative T . By denoting the combined electric field for $T > 0$ as $E_T(t)$ and that for $T < 0$ as $E_{-T}(t)$, the relationship between them can be written as $E_T(-\tilde{t}) = -E_{-T}(\tilde{t})$ from Eq. (9) when $N = 10$. Note that $\tilde{t} = t - t_0$, and t_0 is the antisymmetric center time of the electric field $E_1(t)$ when $N = 10$. Then, we have $A_T(-\tilde{t}) = A_{-T}(\tilde{t})$ for the vector potential. Finally, we get the symmetry of the total energy, namely, $\omega_T(-\tilde{t}) = \omega_{-T}(\tilde{t})$. Similar to the discussion in

Ref. [32], it is easy to find the symmetry of the semiclassical turning point distribution under the transformation $T \rightarrow -T$ in the framework of the Wentzel-Kramers-Brillouin approach. This implies the symmetry between the distribution function for positive T and that for negative T at infinity. The symmetry of the distribution function can also be verified by numerical computation, which is not presented here. A similar verification can also be found in the contents on page 40 of Ref. [30]. Therefore, we can achieve the symmetry of particle number density on the electric-field time interval from Eq. (8). According to the above results, it is easy to find that, to obtain a high number density, the time interval between the strong and slowly varying electric-field pulse train $E_1(t)$ and the weak and rapidly changing one $E_2(t)$ should be zero. This is similar to the result of Ref. [23] for a single-pulse electric field.

B. Full momentum space

In this subsection, we study the EP pair production by combining the multiple-slit interference effect with the DAMS for the full momentum space. The momentum spectra of created particles for the combined electric field $E(t)$ with different pulse numbers are shown in Fig. 6. The pulse number N is chosen as 1, 2, 3, and 10, respectively. We can see that for the single-pulse electric field, i.e., $N = 1$, there is no interference effect, while for $N > 1$, the interference effect is remarkable. Furthermore, when the

electric field pulse number N increases, the region of EP pair production obviously shrinks, but the maximum value of the distribution function $f(\mathbf{k}, +\infty)$ is still about N^2 times that for the single-pulse electric field. Meanwhile, for a large pulse number, there is a pronounced ringlike structure in momentum spectra. From the viewpoint of scattering problem discussed in the above subsection, the resonance effects depend not only on the shape of the finite periodic potential $-[k_{\parallel} - eA(t)]^2$ but also on the incident energy $m^2 + \mathbf{k}_{\perp}^2$. Accordingly, some suitable values of the transverse momentum will give rise to resonances so that the EP pair production can be greatly amplified. Furthermore, for a finite periodic potential, an energy band structure will form, in which the transmission is possible in each allowed band and impossible in each forbidden band [33]. Since the change of the longitudinal momentum k_{\parallel} also influences the shape of the effective potential, the ringlike structure is the result of resonances from both the transverse momentum and the longitudinal momentum. Additionally, we can see that, in contrast to the symmetric momentum spectra for the odd-pulse electric field, the momentum spectra for the even-pulse electric field are asymmetric. This result is related to the symmetry of the electric field, which decides the symmetry of the total energy $\omega(\mathbf{k}, t)$ and finally decides the symmetry of the distribution function $f(\mathbf{k}, +\infty)$; see Ref. [32].

The results mentioned above can also be found from the momentum spectra for the strong and slowly varying alternating-sign electric-field pulse train $E_1(t)$ (see Fig. 7) and for the weak and rapidly varying one $E_2(t)$ (see Fig. 8). However, there are still some new phenomena. First, in Fig. 7, we find that for the large electric field pulse number N the values of distribution function corresponding to the small momentum are very small. Second, in Fig. 8, the cellular structure of the distribution function $f(\mathbf{k}, +\infty)$ is presented and becomes more obvious for a large pulse number [34]. Third, Figs. 7 and 8 clearly show the difference of the multiple-slit interference effect between the nonperturbative Schwinger mechanism and the perturbative multiphoton EP pair production. These results exhibit distinctly nonlinear behaviors, and the deeper underlying physical reasons need further study in the future.

Now, let us consider the number density of created particles $n(+\infty)$ changing with the electric-field pulse number N for the full momentum space. The results are plotted in Fig. 9 for the electric field $E_1(t)$ (dotted blue line), the electric field $E_2(t)$ (dashed red line), and the combined electric field $E(t)$ (solid black line), respectively. First, we can see that the number density $n(+\infty)$ grows with the pulse number N , and the EP pair production is strongly enhanced by combining the multiple-slit

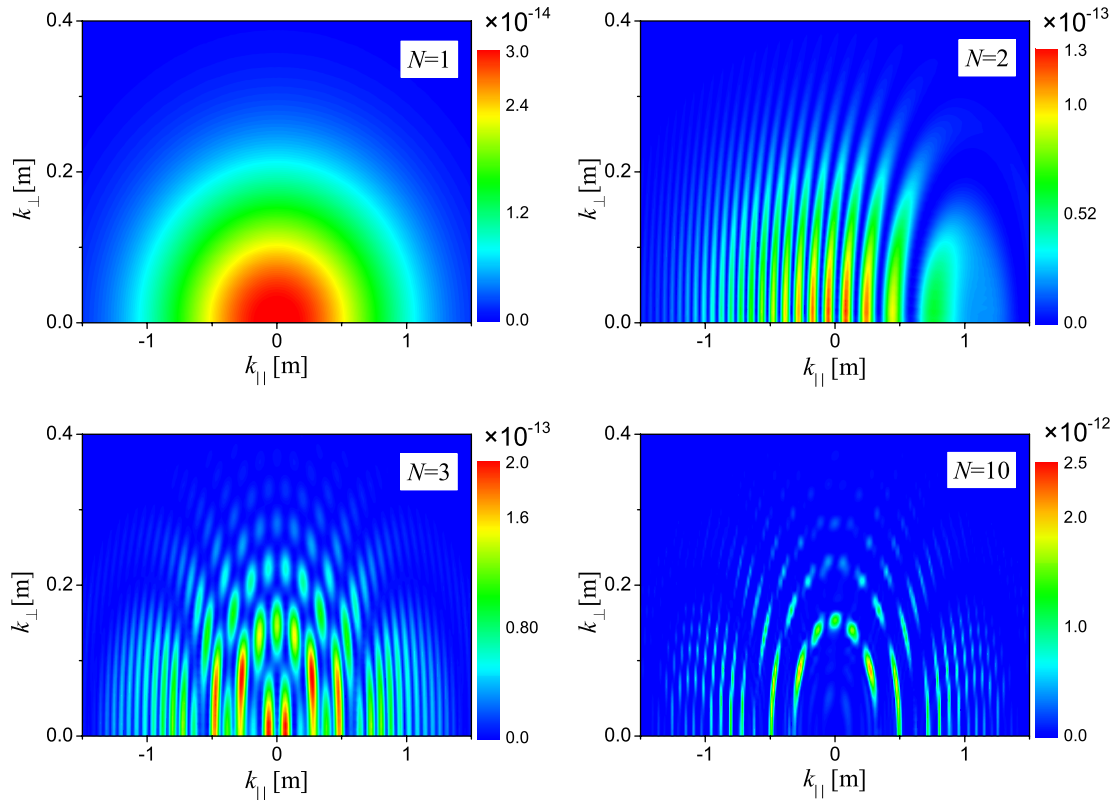


FIG. 7 (color online). The momentum spectra for the strong and slowly varying alternating-sign electric-field pulse train $E_1(t)$ with different electric-field pulse numbers N , i.e., $N = 1, 2, 3$, and 10 . The electric-field parameters are chosen as $E_1 = 0.1$, $\omega_1 = 0.02$, and $\tau = 400.3$.

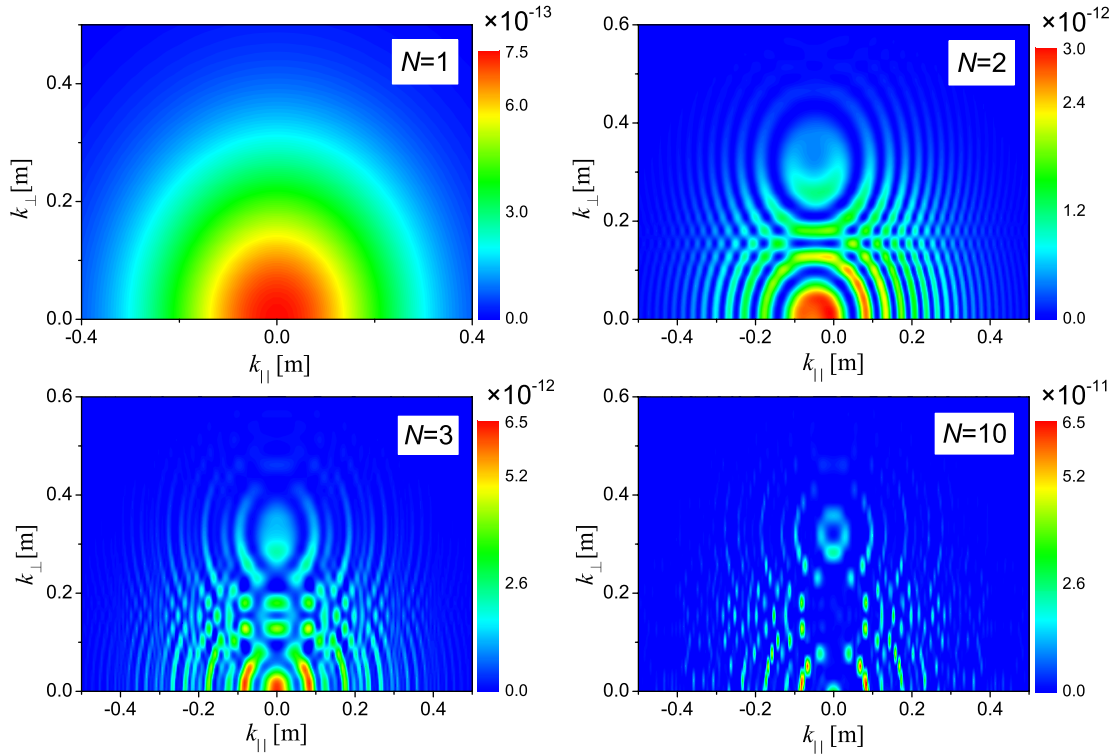


FIG. 8 (color online). The momentum spectra for the weak and rapidly changing alternating-sign electric-field pulse train $E_2(t)$ with different electric-field pulse numbers N , i.e., $N = 1, 2, 3$, and 10 . The electric-field parameters are chosen as $E_2 = 0.01$, $\omega_2 = 0.22$, and $\tau = 400.3$.

interference effect with the DAMS. Second, we find that by considering the contribution of transverse momentum \mathbf{k}_\perp the relationship between the number density $n(+\infty)$ and the pulse number N satisfies a power law with index 1, i.e., a linear relationship. This relationship is different from that shown in Fig. 3, where $\mathbf{k}_\perp = 0$. Third, although the momentum region of pair production shrinks with the increase of the electric-field pulse number, the contribution

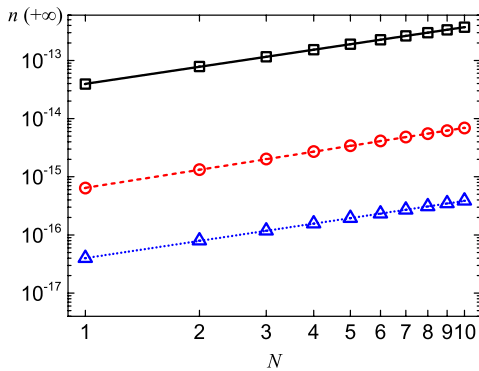


FIG. 9 (color online). The number density of created pairs $n(+\infty)$ as a function of the electric-field pulse number N , for the electric field $E_1(t)$ (dotted blue line), the electric field $E_2(t)$ (dashed red line), and the combined electric field $E(t)$ (black solid line), respectively. The electric-field parameters are the same as in Fig. 1.

of transverse momentum is obvious and worth being considered. Since we are more concerned with the total number of created particles, these results will give us an intuitive picture about the enhanced pair production.

Figure 10 shows the number density $n(+\infty)$ changing with the interpulse time delay τ for the combined electric field $E(t)$ with $N = 10$. We can see that the number density of created particles is sensitive to the interpulse time delay

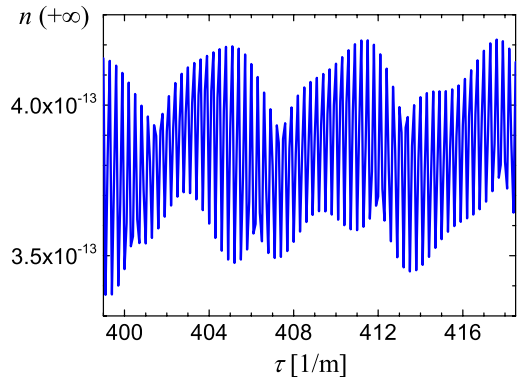


FIG. 10 (color online). The number density of created particles $n(+\infty)$ as a function of the interpulse time delay τ for the combined electric field $E(t)$ with $N = 10$. The electric-field parameters are chosen as $E_1 = 0.1$, $\omega_1 = 0.02$, $E_2 = 0.01$, $\omega_2 = 0.22$, and $T = 0$.

τ , and there is also a quasiperiodic structure. Note that the quasiperiodic structure is more complex than that for vanishing transverse momentum and should be understood as the contribution of resonances from not only the interpulse time delay and the longitudinal momentum but also the transverse momentum. Moreover, the fluctuation amplitude of the number density $n(+\infty)$ is very small and much below 1 order of magnitude compared to that of case with zero transverse momentum.

IV. CONCLUSIONS AND DISCUSSIONS

In summary, in this paper, the EP pair production for the combined electric-field pulse train composed of a strong and slowly varying alternating-sign electric-field pulse train $E_1(t)$ and a weak and rapidly changing one $E_2(t)$ is investigated. It is found that the pair production can be strongly enhanced by combining the multiple-slit interference effect with the DASM. Moreover, the relationship between the number density of created particles and the electric field pulse number is studied for both the vanishing transverse momentum space and the full momentum space. It is shown that for the full momentum space the relationship satisfies a power law with index 1, namely, a linear relationship. The momentum spectra of created particles are also shown for the electric field $E_1(t)$, the electric field $E_2(t)$, and the combined electric field $E(t)$. Their symmetry is related to the symmetry of the external electric fields. After considering the contribution of transverse momentum to EP pair production for the multiple-slit interference effect, which is always neglected for simplifying the numerical computation, the momentum spectra for the

odd-pulse electric field are also discussed. In addition, the effects of interpulse time delay on the EP pair production are studied. It is found that the number density of created particles is very sensitive to the interpulse time delay, and the change of the number density is very small and much below 1 order of magnitude compared to the result for the zero transverse momentum space.

These results are valuable to obtain a high particle number created from vacuum by adjusting the shape of background electric field. They are also helpful for the future experiments aiming at the detection of EP pair production. Additionally, the underlying physical mechanisms for the obvious nonlinear behaviors of momentum spectrum, especially for the cellular structure, still need further study. To optimize the EP pair production, other combined forms of the multiple-slit interference effect and the DASM require further research as well. Obviously, these issues are beyond the scope of this paper and need further study in the future.

ACKNOWLEDGMENTS

This work was supported by the National Natural Science Foundation of China (NSFC) under Grants No. 11175023 and No. 11335013 and also supported partially by the Open Fund of National Laboratory of Science and Technology on Computational Physics at IAPCM and the Fundamental Research Funds for the Central Universities (FRFCU). The numerical calculation was carried out at the HSCC of the Beijing Normal University.

-
- [1] F. Sauter, *Z. Phys.* **69**, 742 (1931).
 - [2] W. Heisenberg and H. Euler, *Z. Phys.* **98**, 714 (1936).
 - [3] J. Schwinger, *Phys. Rev.* **82**, 664 (1951).
 - [4] S. P. Kim and D. N. Page, *Phys. Rev. D* **65**, 105002 (2002); **75045013** (2007).
 - [5] E. Brezin and C. Itzykson, *Phys. Rev. D* **2**, 1191 (1970).
 - [6] G. V. Dunne and C. Schubert, *Phys. Rev. D* **72**, 105004 (2005); C. K. Dumlu and G. V. Dunne, *Phys. Rev. D* **84**, 125023 (2011).
 - [7] Y. Kluger, E. Mottola, and J. M. Eisenberg, *Phys. Rev. D* **58**, 125015 (1998).
 - [8] S. Schmidt, D. Blaschke, G. Röpke, S. A. Smolyansky, A. V. Prozorkevich, and V. D. Toneev, *Int. J. Mod. Phys. E* **07**, 709 (1998).
 - [9] D. V. Vinnik, A. V. Prozorkevich, S. A. Smolyansky, V. D. Toneev, M. B. Hecht, C. D. Roberts, and S. M. Schmidt, *Eur. Phys. J. C* **22**, 341 (2001).
 - [10] R. Alkofer, M. B. Hecht, C. D. Roberts, S. M. Schmidt, and D. V. Vinnik, *Phys. Rev. Lett.* **87**, 193902 (2001).
 - [11] C. D. Roberts, S. M. Schmidt, and D. V. Vinnik, *Phys. Rev. Lett.* **89**, 153901 (2002).
 - [12] F. Hebenstreit, R. Alkofer, and H. Gies, *Phys. Rev. D* **82**, 105026 (2010).
 - [13] <http://www.extreme-light-infrastructure.eu/>.
 - [14] A. Ringwald, *Phys. Lett. B* **510**, 107 (2001).
 - [15] G. V. Dunne, *Eur. Phys. J. D* **55**, 327 (2009).
 - [16] A. Di Piazza, C. Müller, K. Z. Hatsagortsyan, and C. H. Keitel, *Rev. Mod. Phys.* **84**, 1177 (2012).
 - [17] R. Schutzhold, H. Gies, and G. V. Dunne, *Phys. Rev. Lett.* **101**, 130404 (2008).
 - [18] A. R. Bell and J. G. Kirk, *Phys. Rev. Lett.* **101**, 200403 (2008).
 - [19] A. Di Piazza, E. Lötstedt, A. I. Milstein, and C. H. Keitel, *Phys. Rev. Lett.* **103**, 170403 (2009).
 - [20] G. V. Dunne, H. Gies, and R. Schutzhold, *Phys. Rev. D* **80**, 111301 (2009).
 - [21] S. S. Bulanov, V. D. Mur, N. B. Narozhny, J. Nees, and V. S. Popov, *Phys. Rev. Lett.* **104**, 220404 (2010).

- [22] A. Monin and M. B. Voloshin, *Phys. Rev. D* **81**, 025001 (2010).
- [23] M. Orthaber, F. Hebenstreit, and R. Alkofer, *Phys. Lett. B* **698**, 80 (2011).
- [24] C. Fey and R. Schutzhold, *Phys. Rev. D* **85**, 025004 (2012).
- [25] F. Hebenstreit, R. Alkofer, G. V. Dunne, and H. Gies, *Phys. Rev. Lett.* **102**, 150404 (2009).
- [26] A. Nuriman, B. S. Xie, Z. L. Li, and D. Sayipjamal, *Phys. Lett. B* **717**, 465 (2012); N. Abdukerim, Z. L. Li, and B. S. Xie, *Phys. Lett. B* **726**, 820 (2013).
- [27] C. Kohlfürst, M. Mitter, G. von Winckel, F. Hebenstreit, and R. Alkofer, *Phys. Rev. D* **88**, 045028 (2013).
- [28] E. Akkermans and G. V. Dunne, *Phys. Rev. Lett.* **108**, 030401 (2012).
- [29] Z. L. Li, D. Lu, and B. S. Xie, *Phys. Rev. D* **89**, 067701 (2014).
- [30] C. Kohlfürst, Master's thesis, Graz University, 2012, arXiv:1212.0880.
- [31] C. K. Dumlu and G. V. Dunne, *Phys. Rev. Lett.* **104**, 250402 (2010).
- [32] C. K. Dumlu and G. V. Dunne, *Phys. Rev. D* **83**, 065028 (2011).
- [33] D. W. L. Sprung, H. Wu, and J. Martorell, *Am. J. Phys.* **61**, 1118 (1993); R. G. Newton, *ibid.* **62**, 1042 (1994); S. K. Lamoreaux, *ibid.* **64**, 175 (1996).
- [34] D. Blaschke, B. Kämpfer, A. Panferov, A. Prozorkevich, and S. Smolyansky, *Contrib. Plasma Phys.* **53**, 165 (2013).